Nonlinear Dyn (2017) 90:2317–2330
DOI 10.1007/s11071-017-3805-6

ORIGINAL PAPER

Chimera states in ensembles of bistable elements with regular and chaotic dynamics

Igor A. Shepelev · Andrei V. Bukh · Galina I. Strelkova · Tatiana E. Vadivasova · Vadim S. Anishchenko

Received: 6 June 2017 / Accepted: 8 September 2017 / Published online: 18 September 2017

Abstract We consider ensembles of bistable elements with nonlocal interaction. It is shown that the bistability of units in the case of nonlocal interaction leads to the formation of chimera structures of a special type, which we have called double-well chimeras. Their distinctive feature consists in the formation of incoherence clusters with an irregular distribution of elements between two attractive sets existing in an individual element (two "potential wells"). Ensembles of different bistable units are considered, namely ensembles of cubic maps, FitzHugh–Nagumo oscillators in the regime of two stable equilibrium points and Chua's circuits. The spatiotemporal behavior of the ensembles is studied in the cases of regular and chaotic dynamics in time, and different types of chimera structures are revealed.

I. A. Shepelev (✉) · A. V. Bukh · G. I. Strelkova · T. E. Vadivasova · V. S. Anishchenko
Saratov National Research State University, Astrakhanskaya Street 83, Saratov, Russia 410012
e-mail: igor_sar@li.ru

A. V. Bukh
e-mail: buh.andrey@yandex.ru

G. I. Strelkova
e-mail: strelkovagi@info.sgu.ru

T. E. Vadivasova
e-mail: vadivasovate@yandex.ru

V. S. Anishchenko
e-mail: wadim@info.sgu.ru

Keywords Ensemble of oscillators · Spatial structure · Chimera · Dynamical chaos · Nonlocal coupling · FitzHugh–Nagumo oscillator

Mathematics Subject Classification 34G20 · 37N30

1 Introduction

Typically, a bistable system is characterized by two stable states. A system with two stable equilibrium points is the simplest example of a bistable oscillator. The bistable behavior is typical for many issues of physics [1,2], radio-electronics [3], chemistry [4,5], biology [6,7], and other scientific fields [8–11].

Coupled bistable oscillators can form an active bistable medium, where an auto-wave process of the switching type exists [12,13]. Stable traveling waves have been observed in bistable systems and media for specific conditions [14–17]. Bistable media and ensembles of bistable elements are characterized by the formation of spatial structures, both regular and irregular ones. Similar structures have been described, for instance, in [13,18–21].

A new type of structures, which was called a chimera state, has been found and intensively studied in recent years (for instance, [22–28]). A chimera structure consists of clusters with coherent and incoherent behavior. These structures have been revealed for the cases of nonlocal, local [32–34] and global [29–31] coupling between the ensemble elements. Recently, chimeras

have been found in systems with specific kinds of the nonlocal coupling [35–37].

Chimera states are observed in ensembles which consist of active dynamical systems of different types. They can be phase oscillators [27,29,38,39], periodic self-sustained oscillators [25,30,40,41], chaotic self-sustained oscillators and maps [24,28,42–44], and stochastic excitable oscillators [45].

The problem of how chimeras can be related to multistability is one of the important issues. It can be argued that certain chimera types such as chimera "death" [25,46] and a phase chimera in ensembles of chaotic systems [24,28,42–44] appear as a result of the element interaction. Probably, chimera structures are typical states for ensembles consisting of elements with multistability. However, spatial structures in ensembles of multistable oscillators with the nonlocal interaction have not almost been studied. We can note the works [47–49] where chimera states have been explored in ensembles consisting of elements with the bistable dynamics. However, the features of chimera structures, which are exactly related to bistability, have not almost been examined.

Our present paper is devoted to the study of complex spatiotemporal structures in ensembles of bistable elements with the nonlocal coupling. We intend to explore different types of bistable systems, namely a cubic map, the FitzHugh–Nagumo oscillator in the bistable regime, and Chua's circuit. In our research we consider two cases, namely the chaotic dynamics of partial systems and the regime with two stable equilibrium points. The objectives of this paper are to find the general features of an ensemble, which can be related to the bistable dynamics, and to analyze the peculiarities of structure formation in dependence on the dynamics of ensemble elements and the parameters of nonlocal coupling. All the ensembles under study have periodic boundary conditions. Each element of the ensembles interacts with P neighbors both from the left and from the right. We explore the systems with $N = 300$ elements.

2 Chimera states in ensembles of bistable elements with regular dynamics

It is known that certain systems can demonstrate both regular and chaotic bistable dynamics depending on their parameters. Moreover, the chaotic attractor merging can be one of the possible dynamical regimes of such systems. In this section, we explore spatial structures in ensembles of nonlocally coupled cubic maps or FitzHugh–Nagumo (FHN) oscillators in the bistable regime with two symmetrically located equilibrium points.

2.1 Chimeras in an ensemble of bistable maps with regular dynamics

We start with considering an ensemble where a partial unit is a cubic map. This map is the simplest element with the bistable dynamics (see, for example, [50]). The model under study is described by the following system of equations:

$$\begin{aligned} x_i(n+1) &= f_i(n) + \frac{\sigma}{2P}\sum_{k=i-P}^{i+P}\left(f_k(n) - f_i(n)\right), \\ f_i(x) &= \left(\alpha x_i - x_i^3\right)\exp\left[-\frac{x_i^2}{\beta}\right], \quad i = 1,\ldots,N, \\ x_{i+N}(n) &= x_i(n), \quad x_{i+N}(n) = x_i(n), \end{aligned} \tag{1}$$

where the index i defines the element location. This quantity can be considered as a discrete spatial coordinate, n is the iteration number, α, β are the control parameters of a partial element, σ is the coupling strength, and P is the number of neighbors coupled with the ith element from each side. The parameter β is fixed and equal to 10. The coupling radius is specified as $r = \frac{P}{N}$ and characterizes the degree of spatial interaction.

At the beginning of the ensemble Eq. (1) study, we set the parameter $\alpha = 2$. This case corresponds to the regular dynamics of the partial element when the cubic map has two stable equilibrium points. For simplicity, we introduce the term of a "potential well" by analogy with a bistable oscillator such as the Duffing oscillator [2]. It is assumed that the stable equilibrium state in the positive value region of x_i corresponds to a positive well and the negative value region is relevant to a negative well.

In order to illustrate the system behavior, we plot a regime map in the (r, σ) parameter plane in Fig. 1. The regimes are considered for several realizations of initial conditions randomly distributed in the interval $[-1{:}1]$ (i.e., the initial conditions are distributed roughly equal between the two wells). If all the initial conditions

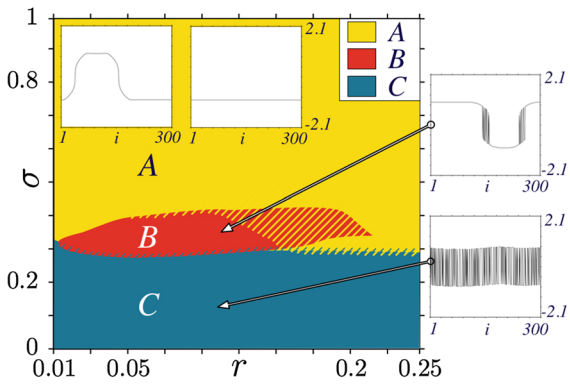

Fig. 1 (Color online) Regime map for the system Eq. (1) in the (σ, r) parameter plane. Designations in the diagram: A—spatial coherence, B—chimera "death", C—spatio-incoherent stationary structures. Parameters: $\alpha = 2$, $\beta = 10$, $N = 300$

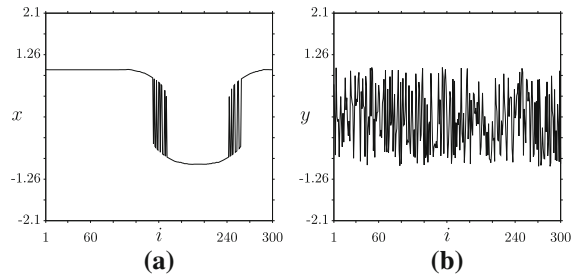

Fig. 2 Stationary chimera structure in the system Eq. (1) for $\sigma = 0.31$ and $r = 0.097$. **a** Snapshot of the system dynamics, **b** realization of the initial conditions randomly distributed between the wells. Parameters: $\alpha = 2$, $\beta = 10$, $N = 300$

belong to one of the wells, then only a spatially uniform regime is observed for any values of r and σ. The boundaries of the system Eq. (1) regimes cannot be exactly defined due to a high-level multistability. For this reason, the same region in the diagram (Fig. 1) can be pictured by both a solid tone and a line alternation. The solid tone means that the regime is realized for all the initial conditions under consideration. The line alternation indicates that in this domain, there coexist two different regimes corresponding to both the main color region and the shaded region.

Only the motionless spatial structures are observed in the ensemble Eq. (1) for the selected parameters and for any values of r and σ. The spatial coherence is realized in region A in the diagram (Fig. 1) for large values of the coupling strength σ. This regime is characterized by a smooth profile which indicates the spatial coherence. At that the spatial structure can be both single-well and double-well. All the elements have the same values corresponding to one of the stable equilibrium points for the single-well spatial structure. When the structure is double-well, then the element values are distributed in the vicinities of the two stable equilibrium points. The coordinates of the element states may be different from the equilibrium point coordinate.

Two scenarios of the spatial structure evolution can be realized when the coupling radius decreases. The first one consists in the transition from region A to region B, where chimera states are observed. Spatial coherence and incoherence clusters can be revealed (see the inset in Fig. 1). They exist only for relatively small values of the coupling radius, which are lower than $\lesssim 0.15$. When r is larger than 0.15, then this regime is realized only for special initial conditions (the region of alternating lines B) and completely disappears with increasing radius r. The transition to region C, which is relevant to irregular stationary spatial structures, occurs when the coupling strength decreases. This is a well-known effect for ensembles of bistable elements with the local coupling (see, for instance, [13,19,20]). The spatial structures are simplified near the region B boundary. The most part of the elements are grouped in the same well. The structure becomes simpler when reducing coupling strength. This behavior is observed for any values of the coupling radius and does not practically change qualitatively within the whole range of r variation.

We now consider region B where stationary chimeras exist. This structure formation is a direct consequence of both the bistability of the system (1) elements and the nonlocal character of coupling. A typical structure which is observed in region B is shown in Fig. 2. Structures with two, four, and even six incoherence clusters coexist for different initial conditions. The multistability disappears with increasing r, and only the structures with two incoherence clusters remain in the system (see Fig. 2a).

2.2 Chimeras in an ensemble of FitzHugh–Nagumo oscillators in the bistable regime

We are interested in whether similar spatial structures observed in the previous case will be formed in an ensemble of continuous-time systems. In order to resolve this issue, we consider an ensemble of coupled FitzHugh–Nagumo oscillators in the bistable regime,

which is described by the following system of differential equations:

$$\begin{aligned} \varepsilon\dot{x}_i &= x_i - \frac{x_i^3}{3} - y_i + \varepsilon\frac{\sigma}{2P}\sum_{k=i-P}^{i+P}(x_k - x_i)\,, \\ \dot{y}_i &= \gamma x_i - y_i - \beta, \\ x_{i+N}(t) &= x_i(t), \quad i = 1, \ldots, N. \end{aligned} \tag{2}$$

Here ε, γ, and β are the control parameters of ensemble elements. The coupling is characterized by the coupling strength σ and the coupling radius $r = \frac{P}{N}$. The Huen method with the step $h = 0.001$ is used for integrating the system (2). The system parameters are selected according to the bistable regime of a partial element, namely $\varepsilon = 0.2$, $\gamma = 0.7$, and $\beta = 0.001$. In this case, there are three equilibrium points in a partial oscillator. They are a saddle and two stable foci. The choice of $\beta = 0.001$ enables one to avoid undesirable effects which are related to the full symmetry of equilibrium points for $\beta = 0.0$. There are no stationary oscillations (both stochastic and periodic ones) in the ensemble element without an external force.

The behavior of the ensemble (2) with the bistable dynamics of the elements and the emergence of a specific type of chimera states have been described in [49]. We now characterize this briefly. Figure 3 illustrates a regime map for the system (2) for fixed values of ε, γ, β in the (r, σ) parameter plane. A set of random initial conditions for the variables x and y within the interval [-1:1] is used for plotting the regime map. This condition means that the oscillators are randomly distributed between the wells in an initial time moment.

The main regimes in the ensemble (2) are periodic traveling waves, a uniform regime (all the elements are in one of the equilibrium states), chimera states, and spatial incoherent stationary structures (regions A, B, C, D in the regime map in Fig. 3, respectively). The typical regimes are shown by the snapshots in the insets.

Periodic traveling waves are propagated in the ring (2) for a strong coupling strength and relatively small values of r. The spatial profile of this wave can be slightly modified both for different initial conditions and when the coupling parameters are varied. The regime of traveling waves is not predominant, i.e., either the traveling wave regime or the equilibrium states can be realized for fixed values of r and σ in the system (2). Chimera structures become to occur for

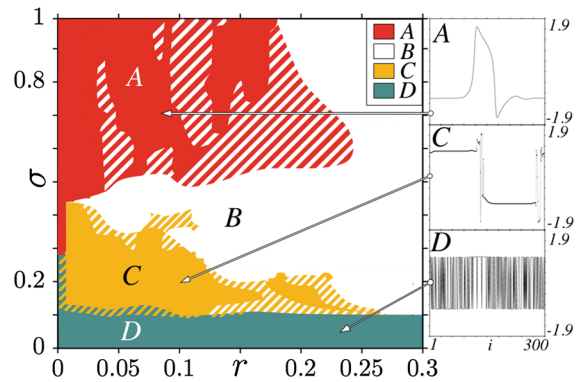

Fig. 3 (Color online) Regime map in the (σ, r) parameter plane. Designations in the map: A—periodic traveling waves, B—equilibrium state, C—chimera states, D—irregular stationary structures. Parameters: $\varepsilon = 0.2$, $\gamma = 0.7$, $\beta = 0.001$, and $N = 300$

the same coupling strength values and with growing coupling radius r. Region B is characterized by the equilibrium state regime for all the ensemble elements. When $r > 0.28$ and $\sigma > 0.1$, this regime is most probable for the majority of initial conditions.

Region C corresponds to the chimera structure existence. In analogue with the previous case, both coherence and incoherence clusters coexist. Moreover, all the elements of the coherence clusters rest in the same equilibrium state. However, the chimera structures in the ensemble (2) significantly differ from the similar structures in the system (1). The chimera structures in the system (2) are not stationary, namely the elements in the incoherence cluster oscillate either within the well (around the cluster edges) or between the equilibrium states (around the cluster center). The spatial distribution of the system elements is irregular. Region D is characterized by irregular spatial structures which are similar to those in (1). The spatial structure is simplified when increasing coupling strength σ. The stationary chimera structure occurs at the chimera region boundaries.

We now consider chimera structures in region C in detail. Coherence and incoherence clusters are well visible in the snapshot of the system dynamics in Fig. 4(a). A set of 30 snapshots at different time moments in Fig. 4(b) demonstrates the temporal dynamics of the ensemble (2).

The elements of coherence clusters are in a resting state and do not oscillate. At least two coherence clusters always exist in a chimera structure. The elements of the first cluster are distributed in one well, and the

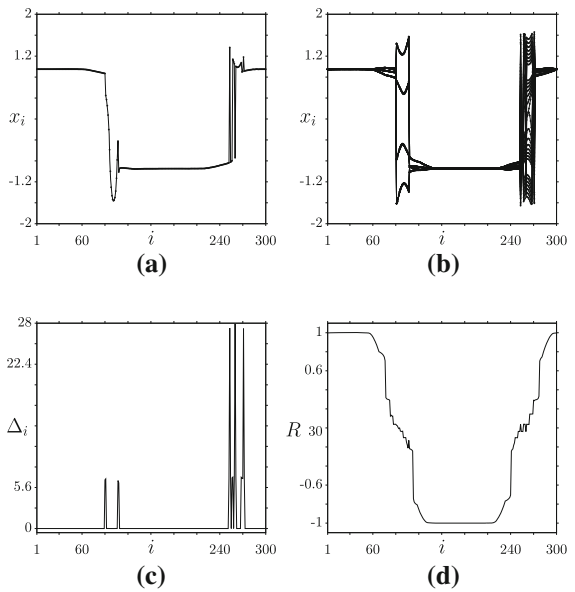

Fig. 4 Chimera structure in the system (2). **a** Snapshot of the system dynamics; **b** set of 30 snapshots at different time moments; **c** root-mean-square deviation of adjacent element states; **d** cross-correlation of the 30th element with the others. The transient time is equal to 10^4 units; the calculation time is equal to 20,000. Parameters: $r = 0.1$, $\sigma = 0.34$, $\varepsilon = 0.2$, $\gamma = 0.7$, $\beta = 0.001$, and $N = 300$

elements of the second cluster are in the other well. Oscillations in the incoherence cluster elements can be only periodic for the value $\beta = 0.001$. Characteristics of the setting regime in region C (Fig. 3) are almost independent of initial conditions unlike the regime in region D.

In order to quantify chimera states, the root-mean-square deviation $\Delta_i(i)$ of element states is calculated by the following formula:

$$\Delta_i = \left\langle (2x_i(t) - x_{i+1}(t) - x_{i-1}(t))^2 \right\rangle, \tag{3}$$

where the angle brackets mean the time averaging. This enables one to estimate the average difference between the instantaneous states of adjacent elements and, thus, to detect the boundaries of coherence and incoherence clusters. The spatial distribution of this characteristic for the chimera state is shown in Fig. 4c. Significant local maxima of Δ_i are observed for the incoherence clusters.

We also calculate the normalized cross-correlation $R_n(i)$ of oscillations of the nth element with other ones by the following formula:

$$R_n(i) = \frac{\langle \tilde{x}_i(t)\tilde{x}_1(t)\rangle}{\sqrt{\langle \tilde{x}_n^2(t)\rangle \langle \tilde{x}_i^2\rangle(t)}}, \qquad \tilde{x}_i(t) = x_i - \langle x_i(t)\rangle. \tag{4}$$

Figure 4d represents a distribution plot for $R_n(i)$ for the 30th oscillator of the chimera structure. The 30th oscillator is located in the incoherence cluster and oscillates with a small amplitude within the positive well. The cross-correlation values are considered equal to ± 1 in regions without oscillations. A cross-correlation sign corresponds to a well where the element is located. Elements around the coherence cluster edges oscillate periodically within a relevant potential well without switchings between the wells. The absolute cross-correlation value decreases for these oscillations. Oscillators from the incoherence cluster switch between the wells. Their $R_n(i)$ values are in the neighborhood of zero due to a very weak interaction between these oscillators and the 30th element. Thus, both characteristics, Δ_i and $R_n(i)$, show well the difference in the behavior between oscillators from both coherence and incoherence clusters. They enable one to clearly detect the cluster boundaries as well as to find regions with different dynamics.

Similar chimera structures are observed when β is close to zero (for instance, $\beta = 0.0001$). However, the behavior of incoherence cluster oscillators can be also chaotic [49]. Thus, the nonlocal interaction leads not only to the occurrence of temporal oscillations in certain localized spatial clusters (as in the case of local coupling [21]) but also to the chimera state formation. This effect is not observed for the case of local interaction.

It can be argued that certain regularities take place in the behavior of ensembles which consist of bistable elements with the regular dynamics. The (r, σ) parameter region, where chimera-like structures are observed, exists for ensembles of different bistable elements. This is characterized by the existence of stable clusters with both regular and irregular spatial distributions. The multistability of chimera states is a feature for both systems. However, there is a significant difference in the behavior of the two systems 2 and 2. The ensemble of cubic maps 2 demonstrates the simplest dynamics, i.e., there are no oscillations for any values of the coupling parameter after a transient process. Stationary structures are only possible. This is the reason of absence of the traveling wave region in the regime map (Fig. 1).

But this region exists in the diagram for the system (2) (Fig. 3). Considerable differences are detected in the element dynamics of both systems in the chimera state region. Stationary chimera structures can only be observed in the system (1). At the same time, one part of the FHN oscillators in the ensemble (2) rests in an equilibrium state and the other part oscillates with different amplitudes. The cluster boundaries are not practically changed in time.

3 Chimeras in an ensemble of bistable elements with chaotic dynamics

We study here two ensembles of bistable elements with chaotic dynamics in analogue with the previous section. The first one is the ensemble of cubic maps described above. However, the element behavior is chaotic in this case. The second model is an ensemble of oscillators which are a radioelectronic device being known as Chua's circuit [3]. The attractor merging bifurcation is a characteristic for both systems and accompanies the transition from bistability to monostability. In this reason, we use initial conditions as a random distribution of the variable values in the interval [0, 1]. Thus, all the elements of the considered ensembles are located only in the positive well at the initial time moment. These initial conditions lead to oscillations only in the positive well, when the regime is bistable. But if a system demonstrates the merged chaotic attractor regime, then the ensemble elements switch between the two wells.

3.1 Chimeras in an ensemble of bistable maps with chaotic dynamics

We now consider the ensemble of nonlocally coupled cubic maps (1). However, we now fix the parameter value $\alpha = 3$ that corresponds to a merged chaotic attractor in a partial map. Other parameters are the same as in the previous case. The effective value of α decreases with increasing coupling strength (see [28]). When we vary the coupling strength, either the merged chaotic attractor regime or bistability is observed in the system. The regime map for the system (1) in the (r, σ) parameter plane is shown in Fig. 5 for $\alpha = 3$, $\beta = 10$. It should be noted that the system has a high-level multistability and sometimes the regime boundaries can have a complex structure.

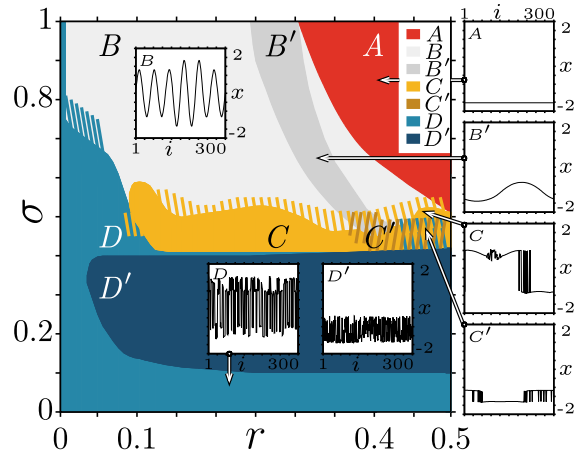

Fig. 5 (Color online) Regime map for the system (1) in the (r, σ) parameter plane. Designation in the map: A—the region of complete chaotic synchronization; B—partial coherence with predominant double-well structures; B′—partial coherence with predominant single-well structures; C—double-well chimeras; C′ – single-well chimeras; D—incoherence double-well structure; D′—incoherence single-well structure. Parameters: $\alpha = 3$, $\beta = 10$, $N = 300$

The regime map demonstrates many types of the spatiotemporal dynamics, which are observed in the ensemble (1) when the parameters r, σ are varied. Some regions in the regimes map (Fig. 5) intersect due to the high-level multistability. These regions are illustrated by alternating lines with different colors according to the color scheme of the regimes. There are also regions with single-well or double-well structures with the same form of oscillations. For simplicity, the regions of the double-well structure existence are denoted by letters without a prime mark and are painted by lighter tones. The regions with single-well structures are marked by letters with a prime mark and are painted by darker tones. Snapshots of the system dynamics demonstrate some typical structures from different regions in Fig. 5.

We now explore the basic types of the spatiotemporal dynamics. They are marked in the regime map (Fig. 5) and in the phase-parametric diagram (Fig. 6). The regions in the phase-parametric diagram are denoted by colors and letters according to the regime map in Fig. 5.

Region A (red color online) corresponds to the complete chaotic synchronization of the elements. The oscillations are chaotic and are associated with the merged attractor. The partial coherence regime is observed in regions B and B' (gray color). Spa-

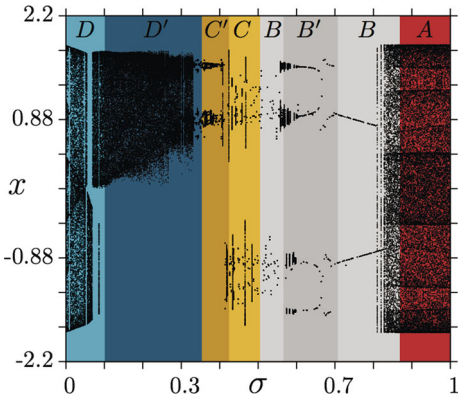

Fig. 6 Phase-parametric diagram of the 50th element in the ensemble (1) for $r = 0.37$ and when varying σ. The regions are indicated by roman numerals (top) and colors according to the same regimes in Fig. 5. Parameters: $\alpha = 3,\ \beta = 10,\ N = 300$

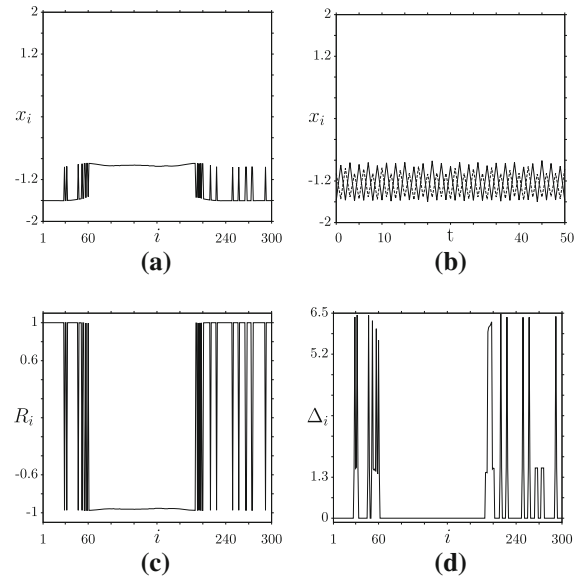

Fig. 7 Single-well chimera structure for $\sigma = 0.43$, $r = 0.42$ (region C' in the regime map in Fig. 5). **a** Snapshot of the system dynamics; **b** time realizations $x_i(n)$ for the 55th and 56th elements from the incoherence cluster; **c** cross-correlation of the first element with the others; **d** root-mean-square deviation of the adjacent element states. The transient time is equal to 10^5 iterations and the calculation time is equal 10^5. Parameters: $\alpha = 3,\ \beta = 10,\ N = 300$

tial structures in these regions are represented smooth profiles and can be either single-well (region B') or double-well (region B). In these regimes, each element demonstrates the single-well chaotic dynamics, even in the case of double-well structures in the ensemble (1) (region B). The partial coherence regime is similar to the complete synchronization near the boundary with region A. The value of $\sigma \approx 0.81$ corresponds to the merging of both chaotic attractors. Each partial map becomes bistable and is in the single-well regime. When the coupling strength decreases up to $\sigma \approx 0.7$, the dynamics of the elements turns out to be periodic.

Regions C and C' are related to chimera structures which can be either double-well (region C) or single-well (region C'). These structures will be considered below. The ensemble elements demonstrate the incoherent behavior in regions D and D' and irregular spatial structures emerge. They are double-well in region D (light-blue color online). At the same time, when $\sigma > 0.05$, each ensemble (1) element oscillates chaotically only in one well. Such a behavior is observed within a wide range of r, σ values. Single-well spatial structures are realized in region D' (dark-blue color online). The ensemble elements behave like uncoupled ones for any values of r and when $\sigma < 0.05$.

We now consider the chimera structures in regions C and C'. Region C' is characterized by the spatially and temporally single-well dynamics. This structure is exemplified in Fig. 7.

A snapshot of the system dynamics $x_i(i)$ is shown in Fig. 7(a). There are clusters with different types of the dynamics. The elements behave synchronously in the coherence cluster. The oscillations are shifted by one iteration within the incoherence cluster. This corresponds to a shift by one half of the period in continuous-time systems. Such a behavior is typical for phase chimeras (see [28,44]).

The ensemble (1) dynamics can be quantified by calculating the following characteristics. At first, the cross-correlation $R_1(i)$ of the first element with the others is estimated by the formula (4). The calculation results are shown in Fig. 7c. Secondly, the root-mean-square deviation Δ_i of the adjacent element states is evaluated by the expression (3) and the corresponding results are presented in Fig. 7d. As can be seen from Fig. 7c, the cross-correlation $R_1(i)$ values are switched between ± 1, i.e., the adjacent elements demonstrate antiphase oscillations. All the elements from the coherence clusters have the same values of $R_1(i)$, which can be either $+1$ or -1 depending on their position. The root-mean-square deviation Δ_i also shows differences in the behavior of the elements from the coherence and incoherence clusters. $\Delta_i \approx 0$ in the coherence cluster

where the elements behave synchronously. At the same time, the values of Δ_i are very large in the incoherence cluster. These characteristics enable one to detect the boundaries of the coherence and incoherence clusters. The cross-correlation and the root-mean-square deviation indicate that this chimera state is a phase chimera.

Double-well chimeras represent a special interest. These regimes dominate in region C in the regime map in Fig. 5. The double-well chimeras are characterized by the following features. The elements of the coherence cluster are located in the same well while ones of the incoherence cluster are in different wells. These structures can appear only in ensembles of bistable elements. Double-well chimeras are not realized for ensembles of another chaotic elements. For instance, this regime cannot be implemented in ensembles of Rössler oscillators or logistic maps. A double-well chimera is exemplified in Fig. 8.

The snapshot of the system dynamics $x_i(i)$ in Fig. 8a exemplifies both double-well and amplitude chimeras. A set of 30 snapshots at different time moments (Fig. 8b) demonstrates the spatiotemporal dynamics of the ensemble (1). All its elements oscillate in one of the wells, without switchings between them. The elements from the amplitude chimera "head" oscillate with a large amplitude in the positive well. The element phases are the same but their instantaneous amplitudes differ from each other. Time realizations for two adjacent elements with the indexes $i = 88, 89$ are plotted in Fig. 8c. As can be seen from the figure, both elements behave chaotically. Figure 8d shows time realizations for two adjacent elements from different wells of the double-well chimera cluster. These elements oscillate irregularly with a small amplitude in the relevant wells.

As before, we calculate the cross-correlation $R_1(i)$ and the root-mean-square deviation Δ_i to quantify the ensemble dynamics. The corresponding plots are shown in Fig. 8e, f. In this case, both characteristics are needed to detect the behavior of the elements from the incoherence clusters. As follows from Fig. 8e, there is a region of $R_1(i)$ values where the amplitude chimera exists and which is characterized by reducing $|R_1(i)| < 1$. The spatial distribution of the Δ_i values (Fig. 8f) indicates a significant difference for the elements from the coherence and incoherence clusters of the double-well chimera. Δ_i is approximately equal to 0 inside the coherence cluster. However, $\Delta_i \ll 0$ for the elements from the double-well chimera "head". At the same time, Δ_i is slightly more than 0 in the amplitude

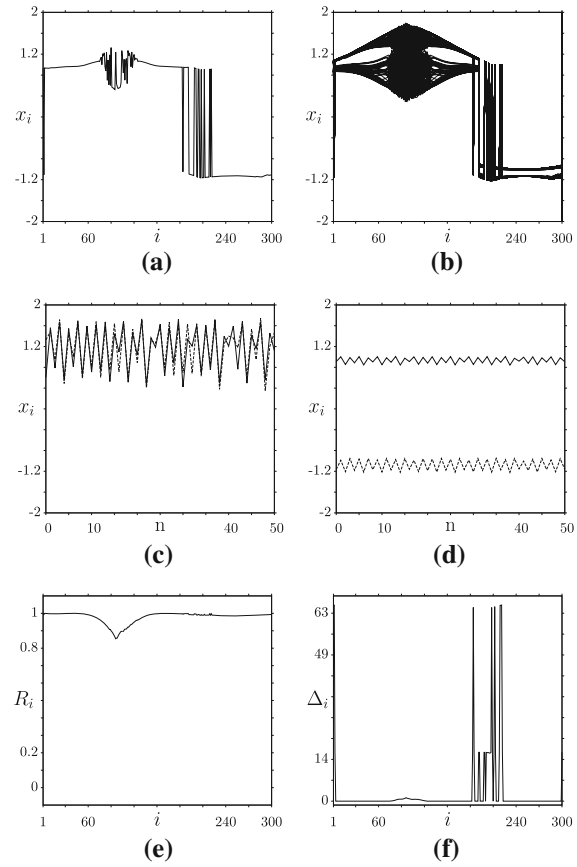

Fig. 8 Double-well chimera for $\sigma = 0.43$, $r = 0.42$ (region C' in the regime map in Fig. 5). **a** Snapshot of the system dynamics; **b** set of 30 snapshots at different time moments; **c** time realizations $x_i(n)$ for the 88th (solid line) and 89th (dotted line) elements from the incoherence cluster; **d** time realizations $x_i(n)$ for the 208th (top solid line) and 209th (bottom dotted line) elements from the incoherence cluster; **e** cross-correlation of the 1st element with the others; **f** root-mean-square deviation of the adjacent element states. The transient time is equal to 10^5 iterations and the calculation time is equal 10^5. Parameters: $\alpha = 3$, $\beta = 10$, $N = 300$

chimera "head". Thus, both characteristics, $R_1(i)$ and Δ_i, are very useful for detecting double-well chimeras.

Eventually, the ensemble of nonlocally coupled chaotic cubic maps demonstrates chimera states. One part of them is already known and has been obtained in ensembles of coupled maps with the Feigenbaum scenario (e.g., the logistic map and the Henon map). The other chimera type is new, and its occurrence is related to the bistable character of ensemble elements. Can similar structures exist in ensembles of continuous-time systems? In order to answer this question, we study an ensemble of nonlocally coupled Chua's oscillators.

3.2 Chimera states in an ensemble of Chua's oscillators with chaotic dynamics

Chua's circuit (Chua's oscillator) can be served as an analogue of the cubic map with chaotic dynamics for continuous-time systems. This circuit represents a radiophysical device. Its features are well explored both numerically and experimentally. We study the behavior of an ensemble of nonlocally coupled Chua's oscillators [51], which is described as follows:

$$\begin{aligned}
\dot{x}_i &= \alpha(y_i - x_i - H(x_i)) + \frac{\sigma}{2P}\sum_{k=i-P}^{i+P}(x_k - x_i)\,,\\
\dot{y}_i &= x_i - y_i - z_i + \frac{\sigma}{2P}\sum_{k=i-P}^{i+P}(y_k - y_i)\,,\\
\dot{z}_i &= -\beta y_i,\\
H(x) &= Bx + \frac{1}{2}(A-B)(|x+1| - |x-1|),\\
x_{i+N}(t) &= x_i(t),\quad y_{i+N}(t) = y_i(t),\\
z_{i+N}(t) &= z_i(t),\quad i = 1,\ldots,N,
\end{aligned} \tag{5}$$

where the index i defines the element location in the ring and can be considered as a discrete spatial coordinate. t is a time moment, α, β, A, and B are the control parameters. σ defines the coupling strength, P is the number of neighbors for the ith element from each side. The following parameters are fixed as $\beta = 14.28$, $A = -1.143$, $B = -0.714$.

The nonlocal interaction leads to the shift of an effective value of the parameter α in an analogue with the ensemble (1). Consequently, the behavior of the system (5) is similar to the cubic map ensemble (1) when the coupling strength increases. As in the previous case, we use the definition of positive and negative wells which correspond to positive and negative values of the variable x, respectively. The definitions of single-well and double-well structures also save the same meaning.

We plot a regime map for the ensemble (5) in the (r, σ) parameter plane for the fixed parameter values $\alpha = 9.4$, $\beta = 14.28$, $A = -1.143$, $B = -0.714$. This is shown in Fig. 9. The boundaries of regimes are obtained by averaging the calculation results for different random initial conditions.

The regime map represents the basic types of the spatiotemporal dynamics which is observed in the ensemble (5) when σ and r are varied. Some regimes in the system (1) coexist due to the high-level multistability. Regions of these regimes are illustrated by alternating

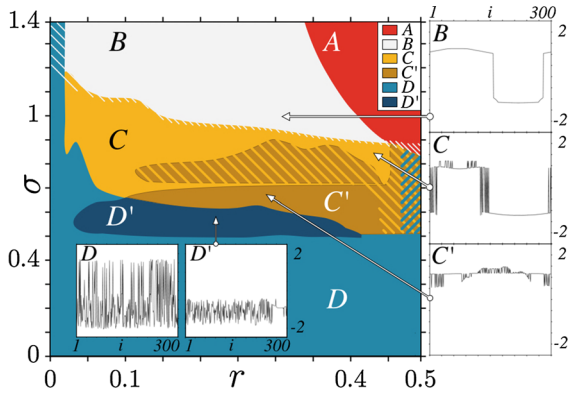

Fig. 9 (Color online) Regime map for the system (5) in the (r, σ) parameter plane. Designations in the map: A—complete chaotic synchronization; B—partial coherence; C—double-well chimera structures; C'—single-well chimera structures; D—full incoherence in double-well structures; D'—full incoherence in single-well structures. Parameters: $\alpha = 9.4$, $\beta = 14.28$, $A = -1.143$, $B = -0.714$, and $N = 300$

lines with tones (color online) relevant to the coexisting regimes. A similar behavior can be observed in both the single-well and double-well structures. For simplicity, the regions of double-well structure existence are denoted by letters without a prime mark and are painted by a lighter tone. The domains of single-well structures are marked by letters with a prime mark and are painted by a darker tone. Snapshots of the system dynamics demonstrate some typical structures which are relevant to different regions in the diagram (Fig. 9).

We now describe the basic types of the spatiotemporal dynamics, which are represented in Fig. 9. A phase-parametric diagram is plotted in Fig. 10 for the 1st element at the fixed coupling radius $r = 0.37$ and when the coupling strength σ is varied. The regions with different regimes in Fig. 10 are denoted by colors and letters in accordance with the regime map in Fig. 9.

The regime which is denoted by letter A (red color) represents complete chaotic synchronization and is implemented only for large values of r. Double-well structures with a smooth profile occur when σ decreases. Thus, there is a partial coherence regime (region B of gray color in the regime map Fig. 9). The chaotic dynamics of the ensemble elements is observed near the complete chaotic synchronization region. The system variables can have both positive and negative values. The dynamics becomes periodic with decreasing σ. Each element oscillates only within its well. However, the spatial distribution remains double-well.

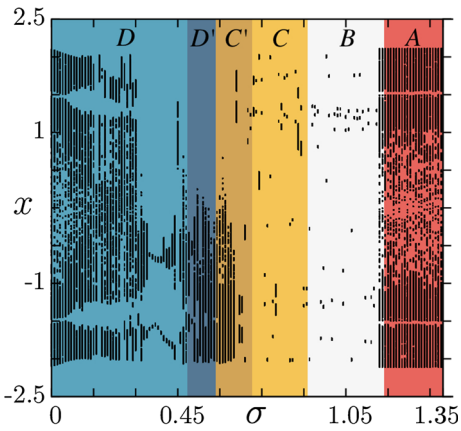

Fig. 10 (Color online) Phase-parametric diagram for the 1st oscillator of the ensemble (5) for $r = 0.37$ and when varying σ. The regions which correspond to different regimes are marked by letters and colors according to the regime map (Fig. 9). Parameters: $\alpha = 9.4$, $\beta = 14.28$, $A = -1.143$, $B = -0.714$, and $N = 300$

It should be noted that this regime always coexists with the complete chaotic synchronization and chimera regimes in the case of very large values of the coupling radius ($r > 0.45$).

Chimera states (yellow regions C and C' in the regime map Fig. 9) appear in the ensemble (5) when the coupling strength decreases further. There are both single-well (region C') and double-well (region C) chimera structures. The oscillator dynamics is predominantly regular or slightly chaotic in the region of double-well chimeras, while it is highly chaotic for most of the single-well structures. At that, the dynamics can be regular around the boundary of regions C and C' (see Fig. 10). The single-well and double-well chimeras coexist in a wide range of parameter r, σ values (alternating lines of light-yellow and dark-yellow colors in regions C and C').

The incoherence regime (desynchronization) is realized in regions D and D' for small values of the coupling strength. There are irregular spatial structures. They can be both single-well (region D') and double-well (region D). The oscillator dynamics is significantly changed with decreasing coupling strength. All the ensemble elements oscillate chaotically in the same well and never switch between the wells. The structures become double-well when σ decreases further. However, the elements remain to oscillate within one well. It is important that there is a narrow range of σ values where the oscillations are periodic. When $\sigma < 0.29$, the temporal oscillations of the elements represent switchings between the wells (the double-scroll regime).

We now consider the ensemble behavior for two cases, namely when the coupling radius values are large, $r > 0.45$, and small, $r < 0.03$. When the interaction between the oscillators is almost global, then it is impossible to detect the region of chimera existence due to the high-level multistability. Both the chimeras and fully irregular structures coexist in the ensemble (5). This region is shown in the diagram (Fig. 9) by alternating lines of blue and yellow colors. If the coupling is almost local, then only double-well irregular structures exist in the system (5). They coexist with partly coherence structures which have complicated but smooth spatial profiles for large values of the coupling strength.

Thus, we can argue that the ensemble of Chua oscillators (5) demonstrates the behavior which is similar to that one of the cubic map ensemble (1).

We now turn to study the chimera states which are realized in the ensemble of chaotic Chua oscillators. We can observe them for both the double-well and single-well structures. At first, we consider the chimera states which exist in region C' in the regime map (Fig. 9). A typical chimera structure is shown in Fig. 11a.

The snapshot of the system dynamics in Fig. 11a shows that clusters with the coherent and incoherent distribution coexist in the ring (5). Oscillations in the coherence cluster are synchronous with the same phase. The structure visibly corresponds to a phase chimera. We now consider the time realization in Fig. 11b for the adjacent elements with indexes 275 and 276 from the chimera "head". Oscillations are periodic, but their phases are shifted on a quarter of the period from each other. In contrary, phase shifts of adjacent oscillators in the incoherence cluster demonstrate an irregular distribution between 0 and $\pi/2$. However, this chimera state is different from the phase chimera which is observed in the ensemble of cubic maps (1), where the phase shift is equal to π.

The cross-correlation (4) and the root-mean-square deviation (3) of the adjacent element states are calculated to quantify the system (5) dynamics. The corresponding plots are shown in Fig. 11c, d. The cross-correlation is calculated for the 1st oscillator from the coherence cluster of the chimera state. Figure 11c indicates that $R_1(i)$ values are equal to 1 inside the coherence cluster. The elements in this cluster oscillate in

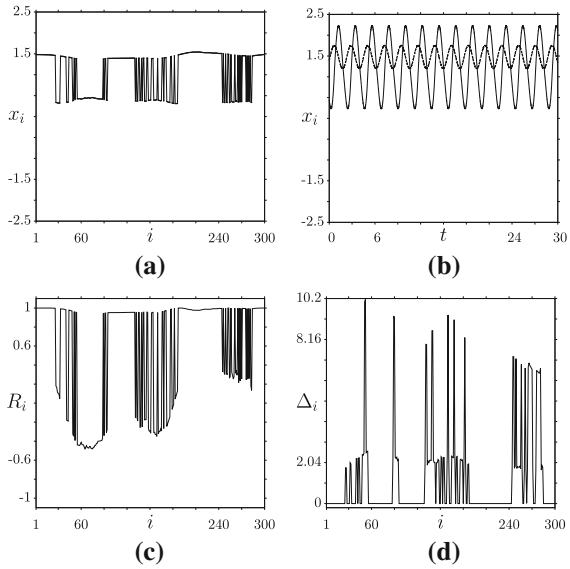

Fig. 11 Single-well chimera structure for $\sigma = 0.75$, $r = 0.37$ (region C' in the regime map in Fig. 9). **a** Snapshot of the system dynamics; **b** time realization $x_i(t)$ for the 275th and 276th elements from the incoherence cluster; **c** cross-correlation of the first element with the others; **d** root-mean-square deviation of the adjacent element states. The transient time is chosen to be 10,000 units, and the calculation time is equal to 5000. Parameters: $\alpha = 9.4$, $\beta = 14.28$, $A = -1.143$, $B = -0.714$, $N = 300$

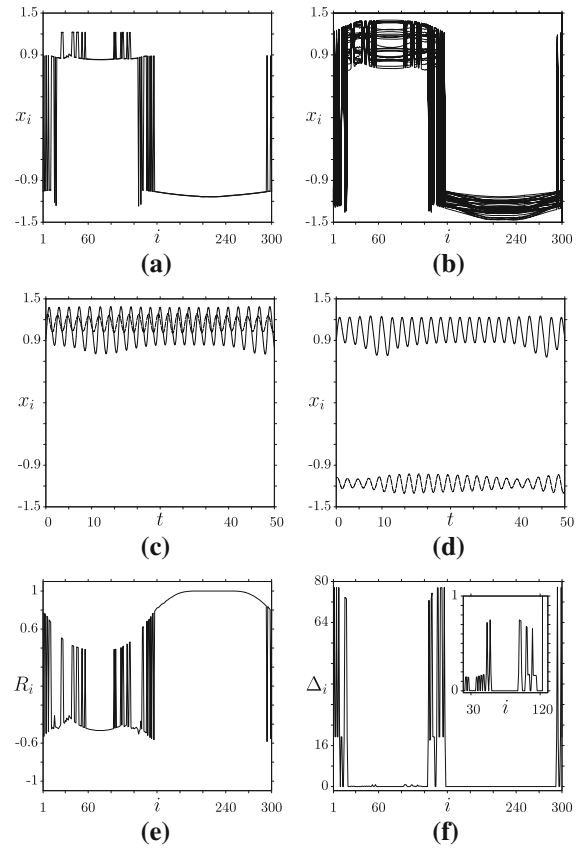

Fig. 12 Double-well chimera for $\sigma = 0.89$, $r = 0.37$ (region C in the regime map in Fig. 9). **a** Snapshot of the system dynamics; **b** set of 30 snapshots at different time moments; **c** time realizations $x_i(t)$ for the 109th (solid line) and 110th (dotted line) elements from the incoherence cluster of the phase chimera; **d** time realizations $x_i(t)$ for the 1st (top solid line) and 2nd (bottom dotted line) elements from the incoherence cluster of the double-well chimera; **e** cross-correlation of the 200th element with the others; **f** root-mean-square deviation of the adjacent element states, the enlarged fragmentary is Δ_i for the phase chimera. The transient time is equal to 10,000 units, and the calculation time is equal 5000. Parameters: $\alpha = 9.4$, $\beta = 14.28$, $A = -1.143$, $B = -0.714$, $N = 300$

phase with the first element. $R_i(i)$ are negative but not equal to -1 for elements from other coherence clusters, which oscillate almost in antiphase with the first element. These values are not exactly equal to -1 because the oscillation amplitudes of elements are different. The values of $R_1(i)$ are irregularly switched between 1 and -1 in the incoherence cluster due to the irregular alternation of oscillation phases. The root-mean-square deviation of the adjacent element states also demonstrates a significantly different behavior of the elements from the coherence and incoherence clusters.

As can be seen in the regime map in Fig. 9, double-well chimeras also exist in the ensemble (5). This chimera type is of special interest because it has not been observed in ensembles of continuous-time systems. A double-well chimera structure from region C in the regime map is shown in Fig. 12a.

Two incoherence clusters which correspond to the phxxxase and double-well chimeras coexist in the same structures. They are shown in Fig. 12a. The first chimera type is located only in one well. The double-well chimera is characterized by an irregular distribution of the oscillators between the wells in the boundary of two adjacent coherence clusters which are located in different wells. Both regimes coexisting in the same structures have already been observed in the ensemble of cubic maps in the previous section. However, the regime in this case has its own distinct features. Figure 12b shows a set of 30 snapshots of the system dynamics over each 10 time units. It is clear that the oscillators are not switched between the wells. The spatial profile does qualitatively change in time. The

time realizations in Fig. 12c, d are plotted for two adjacent elements from incoherence clusters in order to detect the character of chimera states. The adjacent elements from the phase chimera "head" oscillate slightly chaotically in the same well (see Fig. 12c). Moreover, the phases of element oscillations are shifted by $\pi/2$. The oscillations in the incoherence cluster of the double-well chimera differ from those in the ensemble (1). The corresponding time realization is represented in Fig. 12d. The two adjacent elements oscillate in different wells without switchings between the wells. Their amplitudes in various wells differ from each other. The double-well chimera structure in the ring (5) is different from the that one in the ensemble of cubic maps (1). The phases of oscillators from different wells are shifted by $\pi/2$ in the case of the double-well chimera in the ring of Chua's oscillators.

We now calculate the cross-correlation $R_n(i)$ for the 210th element, which is located in the coherence cluster, and the root-mean-square deviation Δ_i of the adjacent element states. Relevant plots are represented in Fig. 12e, f. The cross-correlation enables us to detect both types of chimera states. Positive and negative cross-correlation values are alternated in the incoherence clusters for both the phase and double-well chimera states. The alternating sign $R_n(i)$ is observed due to the phase shift of oscillations from the opposite wells. As in the case of single-well chimera structures, the values of $R_n(i)$ are not exactly equal to ± 1 due to the differences of oscillation amplitudes in various wells. The variance of $R_n(i)$ values for the elements of the double-well chimera is larger than in the case of the phase chimera. The root-mean-square deviation Δ_i of the adjacent element states also enables us to detect incoherence cluster boundaries of double-well chimeras. At the same time, the values of Δ_i for the elements of the phase chimera are less by two orders of magnitude than for the double-well chimera. For this reason, the change is not almost visible in the plot on its scale.

Thus, we indicate that the behavior of the ring of nonlocally coupled Chua's oscillators (5) is qualitatively similar to the dynamics of the ensemble of coupled cubic maps (1). The comparison of two regime maps (see Figs. 9, 5) shows that the basic dynamical regimes of both systems are qualitatively the same. Both systems demonstrate the same chimera structure types including double-well chimeras.

4 Conclusion

We have considered several different models of oscillator ensembles with nonlocal coupling and periodic boundary conditions. The main feature of all the models is the bistable dynamics of ensemble elements. It has been shown that the bistability for the nonlocal interaction leads to the emergence of a special type of the chimera state, which we have referred to as *double-well* chimera structures. Their feature is the incoherence cluster formation. Ensemble elements inside these clusters are irregularly distributed between the neighborhoods of two attractors (two "potential wells") which exist in a partial element. Coherence clusters coexist with the incoherence ones. Elements from them are in the same "well".

Double-well chimera structures are observed both in ensembles of discrete-time systems (maps) and continuous-time systems. The bistability character of a partial element can be different. For the simplest case, a bistable element has two stable equilibrium points. Motionless chimera-like states can be observed for certain values of the coupling parameters in an ensemble which consists of such elements. There are no oscillations in time. These structures are similar to the chimera "death" [25,46] and noticeably differ from irregular spatial structures which exist in ensembles of bistable oscillators with the local coupling [13]. Another difference is the cluster width stability of a double-well chimera toward the change in initial states, in the contrary with the case of irregular structures in ensembles of locally coupled bistable oscillators. This can be explained by the nonlocal interaction and a finite number of ensemble elements. The same chimera state is realized for a sufficiently wide interval of initial conditions. In contrary, the spatial profile structure is fully defined by an initial distribution of ensemble elements between wells in the case of local coupling. A similar behavior is observed in the case of nonlocal coupling when the coupling radius is relatively small. Apparently, there is no clear boundary between the described structure types. These types evolve smoothly one in the other with varying the coupling parameter values.

The ensemble of bistable FHN oscillators shows a more complicated dynamics than the ensemble of bistable maps. Double-well chimeras can be observed in this ensemble. They are not fully motionless, i.e., elements of incoherence clusters oscillate in time. Moreover, these oscillations can be both periodic and

chaotic. The oscillation occurrence in certain element groups in the ensemble of bistable FHN oscillators has been found earlier for the case of local coupling [21]. However, there was no question concerning the chimera structure formation.

In the case of chaotic dynamics of ensemble elements, many different spatiotemporal regimes, including chimera states, can be realized when the coupling parameters are varied. Moreover, the intrawell dynamics becomes possible. This enables us to observe double-well chimeras with the periodic or chaotic temporal behavior, besides motionless ones. It should be noted that single-well chimera structures can occur for certain values of the coupling parameters. They are similar to amplitude and phase chimeras which have been described for ensembles of both continuous-time and discrete-time systems with the Feigenbaum scenario of transition to chaos [24,28,42,44]. This is clear since a sequence of period-doubling bifurcations for each of two coexisting sustainable states is realized in the bistable systems under study. Two samples of ensembles of bistable chaotic elements have been considered in our work, namely the ensemble of cubic maps and the ensemble of Chua's systems. The important fact is that the results obtained for both models coincide. This indicates a universal character of the evolution of similar systems with varying the coupling parameters as well as of the realized types of the spatiotemporal dynamics.

Acknowledgements Sections 2 and 4 were supported by the Russian Science Foundation (Grant No. 16-12-10175). Sections 1 and 3 were supported by the Russian Science Foundation (Grant No. 16-12-10175). This research was partly supported in the framework of SFB910. I. A. Sh. acknowledge support from the Russian Science Foundation (Grant No. 16-12-10175).

References

1. Gibbs, H.M.: Optical Bistability: Controlling Light with Light. Academic Press, Orlando (1985)
2. Haönggi, P., Talkner, P., Borkovec, M.: Reaction-rate theory: fifty years after Kramers. Rev. Mod. Phys. **62**, 251–341 (1990)
3. Madan, R.N.: Chuas Circuit : A Paradigm for Chaos. World Scientific, Singapore (1993)
4. Kramers, H.: Brownian motion in a field of force and the diffusion model of chemical reactions. Physica **7**, 284–304 (1940)
5. Schlögl, F.: Chemical reaction models for nonequilibrium phase-transitions. Z. Phys. **253**, 147–161 (1972)
6. Goldbeter, A.: Biochemical Oscillations and Cellular Rhythms. Cambridge University Press, Cambridge (1997)
7. Izhikevich, E.M.: Dynamical Systems in Neuroscience. The MIT press, Cambridge (2007)
8. May, R.M.: Thresholds and breakpoints in ecosystems with a multiplicity of stable states. Nature **269**, 471–477 (1977)
9. Benzi, R., Sutera, A., Vulpiani, A.: The mechanism of stochastic resonance. J. Phys. A: Math. Gen. **14**, 453–457 (1981)
10. Guttal, V., Jayaprakash, C.: Impact of noise on bistable ecological systems. Ecol. Model. **201**, 420–428 (2007)
11. Benzi, R.: Stochastic resonance: from climate to biology. Nonlinear Process. Geophys. **17**, 431–441 (2010)
12. Mikhailov, S., Loskutov, A.: Foundation of Synergetics. Complex Patterns. Springer, Berlin (1995)
13. Nekorkin, V.I., Velarde, M.G.: Synergetic Phenomena in Active Lattices. Springer, Berlin (2002)
14. Comte, J.C., Morfu, S., Marquié, P.: Propagation failure in discrete bistable reactiondiffusion systems: theory and experiments. Phys. Rev. E **64**, 027102 (2001)
15. Bulsara, A.R., In, V., Kho, A., Longhini, P., Palacios, A., Rappel, W.-J., Acebron, J., Baglio, S., Ando, B.: Emergent oscillations in unidirectionally coupled overdamped bistable systems. Phys. Rev. E **70**, 036103 (2004)
16. Shimizu, K., Endo, T., Ueyama, D.: Pulse wave propagation in a large number of coupled bistable oscillators. IEICE Trans. Fundam. Electr. Commun. Comput. Sci. **91**(9), 2540–2545 (2008)
17. Shepelev, I.A., Slepnev, A.V., Vadivasova, T.E.: Different synchronization characteristics of distinct types of traveling waves in a model of active medium with periodic boundary conditions. Commun. Nonlinear. Sci. and Numer. Simul. **38**, 206–217 (2016)
18. Osipov, G.V., Kurths, J., Zhou, Ch.: Synchronization in Oscillatory Networks. Springer, Berlin (2007)
19. Nekorkin, V.I., Makarov, V.A.: Spatial chaos in a chain of coupled bistable oscillators. Phys. Rev. Lett. **74**, 48194822 (1995)
20. Nekorkin, V.I., Makarov, V.A., Kazantsev, V.B., Velarde, M.G.: Spatial disorder and pattern formation in lattices of coupled bistable elements. Phys. D **100**(3), 330–342 (1997)
21. Nekorkin, V.I., Shapin, D.S., Dmitrichev, A.S., Kazantsev, V.B., Binczak, S., Bilbault, J.M.: Heteroclinic contours and self-replicated solitary waves in a reaction-diffusion lattice with complex threshold excitation. Phys. D **237**(19), 2463–2475 (2008)
22. Kuramoto, Y., Battogtokh, D.: Coexistence of coherence and incoherence in nonlocally coupled phase oscillators. Nonl. Phenom. Complex Syst. **4**, 380–385 (2002)
23. Abrams, D.M., Strogatz, S.H.: Chimera states for coupled oscillators. Phys. Rev. Lett. **93**, 174102 (2004)
24. Omelchenko, I., Maistrenko, Y., Hövel, P., Schöll, E.: Loss of coherence in dynamical networks: spatial chaos and chimera states. Phys. Rev. Lett. **106**, 234102 (2011)
25. Zakharova, A., Kapeller, M., Schöll, E.: Chimera death: symmetry breaking in dynamical networks. Phys. Rev. Lett. **112**, 154101 (2014)
26. Panaggio, M.J., Abrams, D.M.: Chimera states: coexistence of coherence and incoherence in networks of coupled oscillators. Nonlinearity **28**, R67 (2015)

27. Maistrenko, Y., Sudakov, O., Osir, O., Maistrenko, V.: Chimera states in three dimensions. New J. Phys. **17**, 073037 (2015)
28. Bogomolov, S.A., Slepnev, A.V., Strelkova, G.I., Schöll, E., Anishchenko, V.S.: Mechanisms of appearance of amplitude and phase chimera states in a ring of nonlocally coupled chaotic systems. Commun. Nonlinear Sci. Numer. Simul. **43**, 2536 (2016)
29. Yeldesbay, A., Pikovsky, A., Rosenblum, M.: Chimeralike states in an ensemble of globally coupled oscillators. Phys. Rev. Lett. **112**, 144103 (2014)
30. Sethia, G.C., Sen, A.: Chimera states: the existence criteria revisited. Phys. Rev. Lett. **112**, 144101 (2014)
31. Böhm, F., Zakharova, A., Schöll, E., Lüdge, K.: Amplitude-phase coupling drives chimera states in globally coupled laser networks. Phys. Rev. E **91**(14), 040901 (2014)
32. Laing, C.: Chimera in networks with purely local coupling. Phys. Rev. E **92**(5), 050904 (2015)
33. Clerc, M.G., Coulibaly, S., Ferrë, M.A., Garcïa-Nustes, M.A., Rojas, R.G.: Chimera-type states induced by local coupling. Phys. Rev. E **93**, 052204 (2015)
34. Shepelev, I.A., Zakharova, A., Vadivasova, T.E.: Chimera regimes in a ring of oscillators with local nonlinear interaction. Commun. Nonlinear Sci. Numer. Simul. **44**, 277–283 (2016)
35. Laing, C.R., Rajendran, K., Kevrekidis, I.G.: Chimeras in random non-complete networks of phase oscillators. Chaos **22**, 013132 (2012)
36. Hizanidis, J., Panagakou, E., Omelchenko, I., Schöll, E., Hövel, P., Provata, A.: Chimera states in population dynamics: networks with fragmented and hierarchical connectivities. Phys. Rev. E **92**, 012915 (2015)
37. Ulonska, S., Omelchenko, I., Zakharova, A., Schöll, E.: Chimera states in networks of Van der Pol oscillators with hierarchical connectivities. Chaos **26**, 094825 (2016)
38. Abrams, D.M., Mirollo, R., Strogatz, S.H., Wiley, D.A.: Solvable model for chimera states of coupled oscillators. Phys. Rev. Lett. **101**, 084103 (2008)
39. Omelchenko, O.E., Wolfrum, M., Yanchuk, S., Maistrenko, Y.L., Sudakov, O.: Stationary patterns of coherence and incoherence in two-dimensional arrays of non-locally-coupled phase oscillators. Phys. Rev. E **85**, 036210 (2012)
40. Omelchenko, I., Omelchenko, O.E., Hövel, P., Schöll, E.: When nonlocal coupling between oscillators becomes stronger: patched synchrony or multichimera states. Phys. Rev. Lett. **110**, 224101 (2013)
41. Omelchenko, I., Provata, A., Hizanidis, J., Schöll, E., Hövel, P.: Robustness of chimera states for coupled FitzHugh–Nagumo oscillators. Phys. Rev. E **91**, 022917 (2015)
42. Omelchenko, I., Riemenschneider, B., Hövel, P., Maistrenko, Y., Schöll, E.: Transition from spatial coherence to incoherence in coupled chaotic systems. Phys. Rev. E **85**, 026212 (2012)
43. Semenova, N., Zakharova, A., Schöll, E., Anishchenko, V.: Does hyperbolicity impede emergence of chimera states in networks of nonlocally coupled chaotic oscillators? Europhys. Lett. **112**, 40002 (2015)
44. Slepnev, A.V., Bukh, A.V., Vadivasova, T.E.: Stationary and non-stationary chimeras in an ensemble of chaotic self-sustained oscillators with inertial nonlinearity. Nonlinear Dyn. **88**, 1–10 (2017)
45. Semenova, N., Zakharova, A., Anishchenko, V., Schöll, E.: Coherence-resonance chimeras in a network of excitable elements. Phys. Rev. Lett. **117**, 014102 (2016)
46. Banerjee, T., Dutta, P.S., Zakharova, A., Schöll, E.: Chimera patterns induced by distance-dependent power-law coupling in ecological networks. Phys. Rev. E. **94**, 032206 (2016)
47. Dudkowski, D., Maistrenko, Y., Kapitaniak, T.: Different types of chimera states: an interplay between spatial and dynamical chaos. Phys. Rev. E **90**, 032920 (2014)
48. Mishra, A., Hens, Ch., Bose, M., Roy, P.K., Dana, S.K.: Chimeralike states in a network of oscillators under attractive and repulsive global coupling. Phys. Rev. E **92**, 062920 (2015)
49. Shepelev, I.A., Vadivasova, T.E., Strelkova, G.I., Anishchenko, V.S.: New type of chimera structures in a ring of bistable FitzHugh–Nagumo oscillators with nonlocal interaction. Phys. Lett. A **381**(16), 1398–1404 (2017)
50. Scjolding, H., Branner-Jorgensen, B., Christiansen, P.L., Jensen, H.E.: Bifurcations in discrete dynamical systems with cubic maps. SIAM J. Appl. Math. **43**(3), 520–534 (1983)
51. Anishchenko, V.S.: Dynamical Chaos—Models and Experiments, vol. 8. World Scientific, Singapore (1995)